# Critical behavior of the mixed-spin Ising model with two competing dynamics

Mauricio Godoy and Wagner Figueiredo*
*Departamento de Física–Universidade Federal de Santa Catarina, 88040-900, Florianópolis, Santa Catarina, Brazil*
(Received 27 July 2001; revised manuscript received 5 September 2001; published 16 January 2002)

In this work we investigate the stationary states of a nonequilibrium mixed-spin Ising model on a square lattice. The model system consists of two interpenetrating sublattices of spins $\sigma=1/2$ and $S=1$, and we take only nearest neighbor interactions between pairs of spins. The system is in contact with a heat bath at temperature $T$ and subject to an external flux of energy. The contact with the heat bath is simulated by single spin flips according to the Metropolis rule, while the input of energy is mimicked by the simultaneous flipping of pairs of neighboring spins. We performed Monte Carlo simulations on this model in order to find its phase diagram in the plane of temperature $T$ versus the competition parameter between one- and two-spin flips, $p$. The phase diagram of the model exhibits two ordered phases with sublattice magnetizations $m_1$, $m_2>0$ and $m_1>0$, $m_2<0$. These phases are separated from the paramagnetic phase ($m_1=m_2=0$) by continuous transition lines. We found the static critical exponents along these lines and showed that this nonequilibrium model belongs to the universality class of the two-dimensional equilibrium Ising model.

DOI: 10.1103/PhysRevE.65.026111 PACS number(s): 64.60.Ht

## I. INTRODUCTION

Kinetic Ising models on a lattice have been employed to describe the stationary nonequilibrium states of a great variety of problems [1,2]. Aside from the exact solution found by Glauber for the kinetic Ising model in one dimension [3], the majority of studies in this field employ computer simulation methods. The reason for this is the absence of a complete theory concerning nonequilibrium phenomena such as we have for the case of problems considered in equilibrium statistical mechanics.

In this work we consider a particularly simple model of a nonequilibrium system. The model is an Ising system with spin- $\frac{1}{2}$ and spin-1 variables on different sublattices of the square lattice. The time evolution of the states of the system is governed by two competing dynamical processes: one simulating the contact of the system with a heat bath at a temperature $T$, and the other mimicking an input of energy into the system. The contact with the heat bath is simulated by the Glauber [3] stochastic process, where both the $\sigma$ and $S$ spins relax through one-spin flips, with probability $p$, while the input of energy is modeled by flipping a pair of nearest neighbor spins simultaneously, with probability $(1-p)$. Only two-spin flips that increase the energy of the system are permitted in this model. Therefore, the flux of energy into the system favors states of higher energy, causing a competition with the one-spin flip Glauber process. This model has already been studied in the pair approximation [4] and the phase diagram in the $T$-$p$ plane determined. We found two continuous transition lines: one line separating an ordered phase where the sublattice magnetizations are aligned parallel from a disordered phase where the sublattice magnetizations are both zero (paramagnetic phase), and another line separating the paramagnetic phase from an ordered phase where the sublattice magnetizations are aligned in opposite directions. In the pair approximation nearly half of the area of the phase diagram is occupied by the paramagnetic phase, the other half being occupied by the ordered phase with magnetizations in opposite directions. The ordered phase with both magnetizations positive occupies a very small region of the phase diagram.

Each of the dynamical processes we consider satisfies the detailed balance condition, which drives the system toward equilibrium. However, when both act simultaneously, detailed balance is no longer satisfied and the system is forced out of equilibrium. In the present model the two dynamics do not conserve the order parameter. The two-spin flip we consider here is different from the usual Kawasaki kinetics [5] because the two sublattices are not equivalent. Tomé and de Oliveira [6] considered an Ising ferromagnetic system evolving in time according to two competing dynamical processes: the one-spin flip Glauber dynamics, and the two-spin exchange Kawasaki dynamics. They found three different types of magnetic ordering as the competition parameter between these two stochastic processes changes. Ferromagnetic, paramagnetic, and antiferromagnetic phases appear in their phase diagram. Our mixed-spin Ising system also presents three different phases, and this is related to the fact that the two-spin flips in both models increase the energy of the system. However, in their work the two-spin exchange Kawasaki dynamics conserves the order parameter, while in our case this does not happen because the two sublattices are not equivalent.

The phase diagram and the critical properties of Ising systems with competing Glauber and Kawasaki dynamics have been extensively studied in recent years and a review can be found in Ref. [7]. In this work we used Monte Carlo simulations and finite-size scaling arguments [8] to determine the phase transitions and the static critical exponents of the model. We attributed a weight $p$ to the one-spin flip process, and a weight $(1-p)$ to the two-spin flip process. We determined the phase diagram of the model in the plane of temperature $T$ versus competition parameter $p$, and we also noticed the presence of three different phases. For $p\simeq 1$ (small flux of energy) we obtained an ordered phase where the sub-

*Electronic address: wagner@fisica.ufsc.br

 

lattice magnetizations are both positive. On increasing the flux of energy, the ordered phase becomes unstable and a disordered phase (paramagnetic phase) appears. However, for a large value of the flux of energy ($p \simeq 0$), we observe the presence of another ordered phase, whose symmetry is different from that found at large values of $p$. We determined the critical exponents $\nu$, $\beta$, and $\gamma$ along the continuous transition lines, and we showed that the mixed-spin model is in the same universality class as the equilibrium Ising model.

The rest of this paper is organized as follows. Section II describes the mixed-spin Ising model and the two competing dynamical processes. In Sec. III, we give some details concerning the Monte Carlo simulations and define the observables of interest. In Sec. IV we present the results of the simulations, the phase diagram, and the static critical exponents of the model. Finally, in Sec. V, we present our conclusions.

## II. THE MIXED-SPIN ISING MODEL

We consider a mixed-spin Ising model defined in a square lattice of linear size $L$, with spins $\sigma = 1/2$ and $S = 1$. The lattice is bipartite, with the $\sigma$ spins occupying the sites of one sublattice, while the $S$ spins occupy the sites of the other sublattice, each sublattice containing $N$ sites. A state of the system is represented by $\{\sigma,S\} \equiv \{\sigma_1,\ldots,\sigma_l,\ldots,\sigma_N;S_1,\ldots,S_m,\ldots,S_N\}$, where the spin variables $\sigma_l$ can assume the values $\pm 1$ and the spin variables $S$ can assume the values 0, $\pm 1$. The energy of the system in the state $(\sigma,S)$ is given by

$$E(\sigma,S) = -J\sum_{(i,j)} S_i\sigma_j, \tag{1}$$

where the sum is over all nearest neighboring pairs of spins, and $J$ is taken to be positive. Let us denote by $p(\sigma,S;t)$ the probability of finding the system in the state $(\sigma,S)$ at time $t$. The equation of motion for the probability of the states of the system is given by the gain-loss master equation

$$\frac{d}{dt}p(\sigma,S;t) = -\sum_{\sigma,S} W(\sigma,S\to\sigma',S')p(\sigma,S;t) + \sum_{\sigma,S} W(\sigma',S'\to\sigma,S)p(\sigma',S';t), \tag{2}$$

where $W(\sigma,S\to\sigma',S')$ is the probability, per unit of time, for the transition from the state $(\sigma,S)$ to the state $(\sigma',S')$. In this model, we assume that the transition rate $W(\sigma,S\to\sigma',S')$ is given by the competition between two independent stochastic processes: the one-spin flip Glauber process, intended to describe the relaxation of the $\sigma$ and $S$ spins due to the contact with the heat bath at temperature $T$, which can be written in the form

$$W_G(\sigma,S\to\sigma',S') = W_G(\sigma,S\to\sigma',S) + W_G(\sigma,S\to\sigma,S'), \tag{3}$$

and the two-spin flip process, chosen independent of temperature, and designed to increase the energy of the system, which can be written as $W_{\mathrm{GD}}(\sigma,S\to\sigma',S')$. Then, we have the following equation for the total transition probability:

$$W(\sigma,S\to\sigma',S') = pW_G(\sigma,S\to\sigma',S') + (1-p)W_{\mathrm{GD}}(\sigma,S\to\sigma',S'), \tag{4}$$

where $0 \leqslant p \leqslant 1$ is the competition parameter between the one-spin flip and two-spin flip processes. The one-spin flip process is described by the Glauber dynamics, that is,

$$W(\sigma,S\to\sigma',S') = \sum_{j=1}^{N} \delta_{\sigma_1,\sigma_2'}\delta_{\sigma_2,\sigma_2'}\cdots\delta_{\sigma_j,-\sigma' j}\cdots\delta_{\sigma_N,\sigma_N'} \times \delta_{S_1,S_1'}\delta_{S_2,S_2'}\cdots\delta_{S_k,S_k'}\cdots\delta_{S_N,S_N'}\omega_j(\sigma') + \sum_{k=1}^{N} \delta_{\sigma_1,\sigma_1'}\delta_{\sigma_2,\sigma_2'}\cdots\delta_{\sigma_j,\sigma_2'}\cdots\delta_{\sigma_N,\sigma_N'} \times \delta_{S_1,S_1'}\delta_{S_2,S_2'}\cdots\delta_{S_k,\tilde{S}_k}\cdots\delta_{S_N,S_N'}\omega_k(\tilde{S}), \tag{5}$$

where $\omega_j(\sigma)$ and $\omega_k(S)$ are the probabilities of flipping the spins $\sigma_j$ and $S_k$, respectively. We use the variable $\tilde{S}_k$ to mean the two possible values that a change of the actual spin variable $S_k$ can take. We adopt the Metropolis prescription for the one-spin flip transitions, that is,

$$\omega_j(\sigma) = \min[1,\exp(-\beta\Delta E_j)], \tag{6}$$

where $\beta = 1/k_BT$, and $T$ is the absolute temperature of the heat bath. $\Delta E_j$ is the change in energy after flipping spin $\sigma_j$ at site $j$. We also assume a similar expression for $\omega_k(S)$. For the two-spin flip we can write

$$W_{\mathrm{GD}}(\sigma',S'\to\sigma,S) = \sum_{j,k=1}^{N} \delta_{\sigma_1,\sigma_1'}\delta_{\sigma_2,\sigma_2'}\cdots\delta_{\sigma_j,-\sigma_j'}\cdots\delta_{\sigma_N,\sigma_N'} \times \delta_{S_1,S_1'}\delta_{S_2,S_2'}\cdots\delta_{S_k,\tilde{S}_k}\cdots\delta_{S_N,S_N'}\omega_{jk}(\sigma',\tilde{S}), \tag{7}$$

where $\omega_{jk}(\sigma,S)$ is the probability of a simultaneous flipping of the neighboring spins $\sigma_j$ and $S_k$. This process favors an increase in the energy of the system, and it is written as

$$\omega_{jk}(\sigma,S) = \begin{cases} 0 & \text{if } \Delta E_{jk} \leqslant 0 \\ 1 & \text{if } \Delta E_{jk} > 0, \end{cases} \tag{8}$$

where $\Delta E_{ij}$ is the change in energy after flipping the spins $\sigma_j$ and $S_k$ at the neighboring sites $j$ and $k$.

## III. MONTE CARLO SIMULATIONS

We used the standard importance sampling technique to simulate the model introduced in the last section. We considered square lattices of linear size $L$, with values of $L$ ranging from $L = 16$ to 128, and we applied periodic boundary conditions. We have taken completely random spin configurations as the initial states of our simulations. A new configuration is generated from an old one by the following Markov

process: for a given temperature $T$ and a selected value of the competition parameter $p$, we choose at random a spin of the lattice, and then we generate a random number $\xi$ between zero and unity. If $\xi \leqslant p$ we choose to perform the one-spin flip process, according to the Metropolis prescription given by Eq. (6). If $\xi > p$, then we consider the two-spin flip process. In this case, we randomly select a new spin that is a nearest neighbor of the initial chosen spin, and we apply the prescription given by Eq. (8). In general, we discarded the first $5\times10^4$ Monte Carlo Steps (MCS) in order to achieve the stationary regime for all lattice sizes. In order to estimate the quantities of interest, we considered the next $4\times10^5$ MCS to calculate the averages for any lattice size. One MCS equals $L^2$ one-spin flip or two-spin flip trials.

We calculated the sublattice magnetizations per spin, $m_1$ and $m_2$, defined as

$$m_1 = \frac{1}{N}\left\langle \sum_i S_i \right\rangle \tag{9}$$

and

$$m_2 = \frac{1}{N}\left\langle \sum_j \sigma_j \right\rangle. \tag{10}$$

We also defined the total and the staggered magnetizations, respectively, by

$$m^F = |(m_1 + m_2)|, \tag{11}$$

and

$$m^{\mathrm{AF}} = |(m_1 - m_2)|, \tag{12}$$

and their associated reduced fourth-order Binder cumulants [9]

$$U_L(m) = 1 - \frac{\langle m^4 \rangle}{3\langle m^2 \rangle^2}. \tag{13}$$

The corresponding susceptibilities are defined by

$$\chi(m) = N\{\langle m^2 \rangle - \langle |m| \rangle^2\}, \tag{14}$$

where $m$ can be $m^F$ or $m^{\mathrm{AF}}$.

These above defined quantities obey the following finite-size scaling relations in the neighborhood of the stationary critical point $p_c$:

$$m_L(p) = L^{-\beta/\nu} m_0(L^{1/\nu}\epsilon), \tag{15}$$

$$\chi_L(p) = L^{\gamma/\nu} \chi_0(L^{1/\nu}\epsilon), \tag{16}$$

$$U_L(p) = U_0(L^{1/\nu}\epsilon), \tag{17}$$

where $\epsilon = (p - p_c)/p_c$, $p_c$ being the critical competition parameter for each value of $T$.

The derivative of Eq. (17) with respect to the competition parameter $p$ give us the following scaling relation:

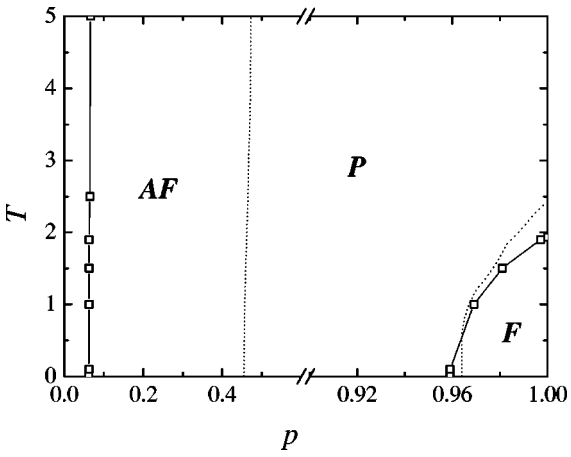


FIG. 1. Phase diagram of the nonequilibrium mixed-spin Ising model in the $T$-$p$ plane. The letters denote the $F$ and AF ordered phases and the paramagnetic $P$ phase. The full lines give the results of simulations, while the dotted lines represent the pair approximation calculation. The temperature is measured in units of $J/k_B$ and $p$ is a dimensionless parameter.

$$U_L'(p) = L^{1/\nu}\frac{U_0'(L^{1/\nu}\epsilon)}{p_c}, \tag{18}$$

so that

$$U_L'(p_c) = L^{1/\nu}\frac{U_0'(0)}{p_c}. \tag{19}$$

We can determine the critical exponent $\nu$ from a log-log plot of $U_L'(p_c)$ versus $L$.

## IV. RESULTS

In Fig. 1 we show the phase diagram of the model in the $T-p$ plane. It displays three different phases, separated by two continuous transition lines: one line separating an ordered phase ($F$), where the sublattice magnetizations are both positive, from a disordered paramagnetic phase ($P$), where both sublattice magnetizations are zero. The other line separates the paramagnetic phase from a different ordered phase (AF), where the sublattice magnetizations are aligned in opposite directions. As we can see, the paramagnetic phase occupies almost all the region of the phase diagram. We also plotted in Fig. 1 the results obtained previously [4] in the pair approximation. In this approximation the AF phase occupies an area of the phase diagram as large as the paramagnetic phase. On the other hand, the $F$ phase occupies a very small area of the phase diagram in both the pair approximation and the Monte Carlo simulations. For the particular case $p=1$, where only one-spin flips are permitted, the stationary state coincides with the thermodynamic equilibrium state, because there is no flux of energy into the system. For $p=1$, the transition temperature between the ordered $F$ phase and the paramagnetic $P$ phase is $T_c = 1.934 \pm 0.007$. This value was found by considering the common point where the cumulants for different lattice sizes cross, as we will show next. However, this point is not exactly the

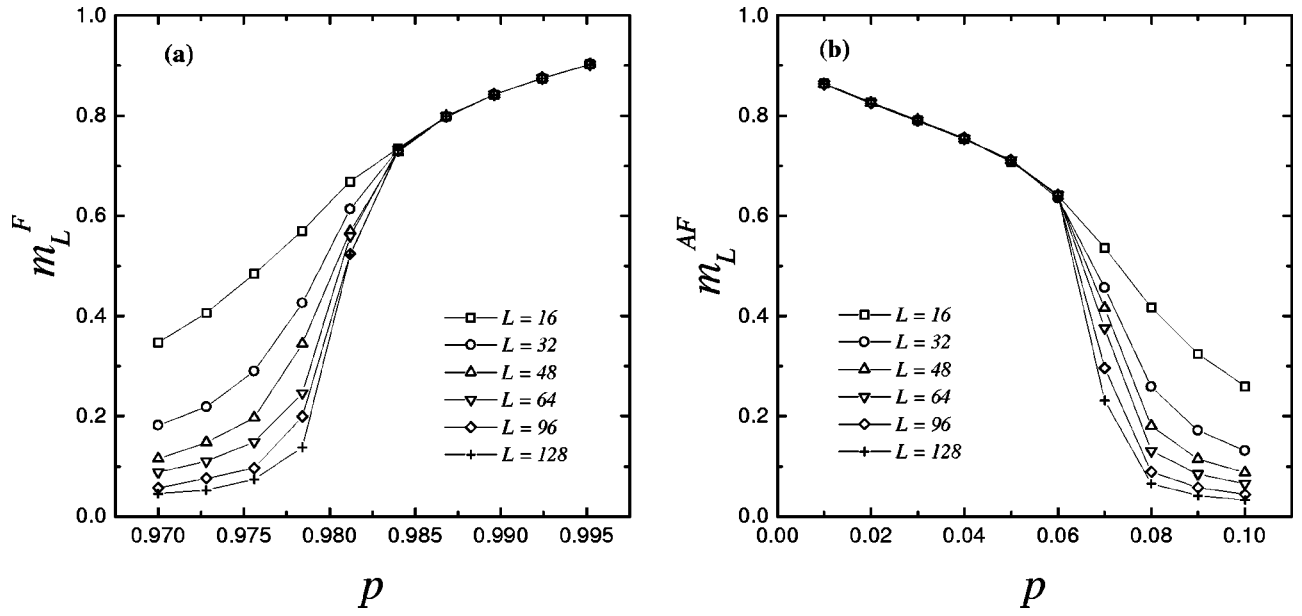


FIG. 2. Finite-size behavior of the order parameters as a function of the competition parameter $p$ for several lattice sizes $L$ indicated in the figures. (a) Total magnetization $m^F$ for $T=1.5$. (b) Staggered magnetization $m^{\mathrm{AF}}$ for $T=2.0$.

same for each pair of lattice sizes in the simulations. The uncertainty is related to the spread of the values of temperature around a mean value, after all the crossing points are considered. Our critical temperature is in good agreement with the one found from series expansion calculations [10], $T_c=1.952$. The temperature is measured in units of $J/k_B$.

The order parameter of the $F$ phase is $m^F$, while the one associated with the ordered AF phase is $m^{\mathrm{AF}}$. These parameters go continuously to zero at the borders of the $F$ and AF phases with the $P$ phase. Figures 2(a) and 2(b) show the behavior of the order parameters $m^F$ and $m^{\mathrm{AF}}$, respectively, as a function of $p$ for various lattice sizes, and at a fixed temperature. Figure 2(a) indicates that the order parameter $m^F$ is of order unity for $p>p_c$ and vanishes for $p<p_c$, except for finite-size effects. The same behavior is also observed for the order parameter $m^{\mathrm{AF}}$ when we cross the transition point [Fig. 2(b)]. We can also get some information concerning the transition point by examining the behavior of the order parameters as a function of $1/L$, as we can see in Figs. 3(a) and 3(b). For instance, in Fig. 3(a), we plotted $m^F$ against $1/L$ for some selected values of $p$ in the range $p=0.9800-0.9830$. From this figure we can say that the criti-

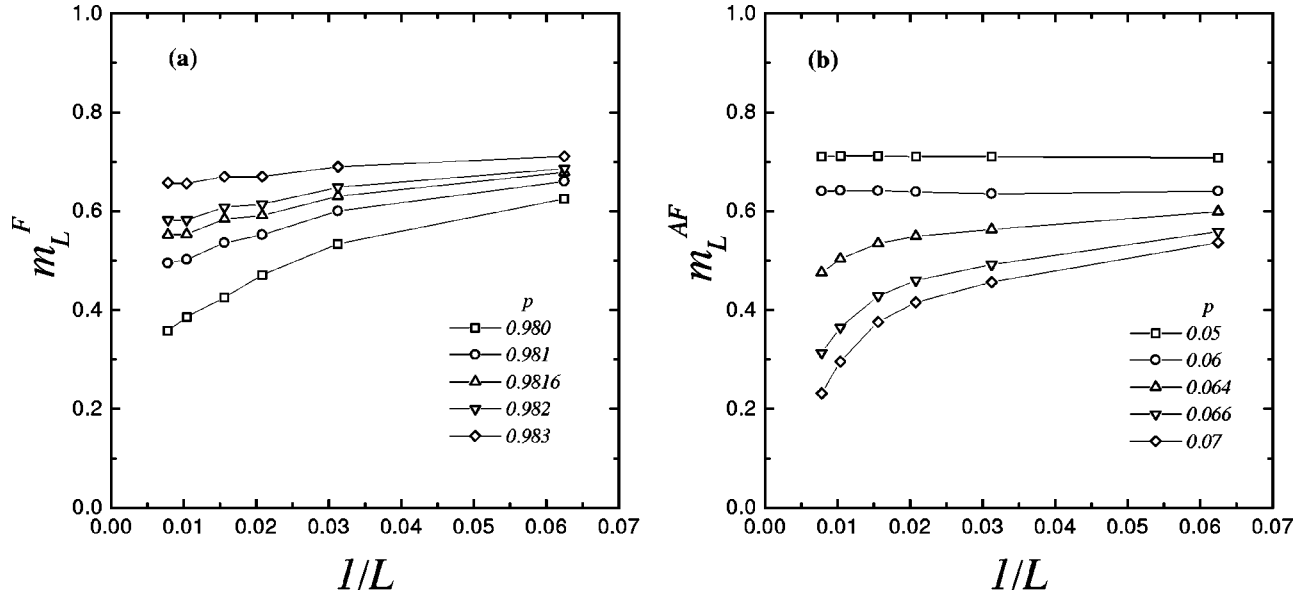


FIG. 3. Magnetization as a function of $1/L$ for several values of the competition parameter $p$ as indicated in the figures. (a) Total magnetization $m^F$ for $T=1.5$; the transition appears to be in the range $0.9810\leqslant p\leqslant 0.9820$. (b) Staggered magnetization $m^{\mathrm{AF}}$ for $T=2.0$; the transition is located in the range $0.06\leqslant p\leqslant 0.07$.

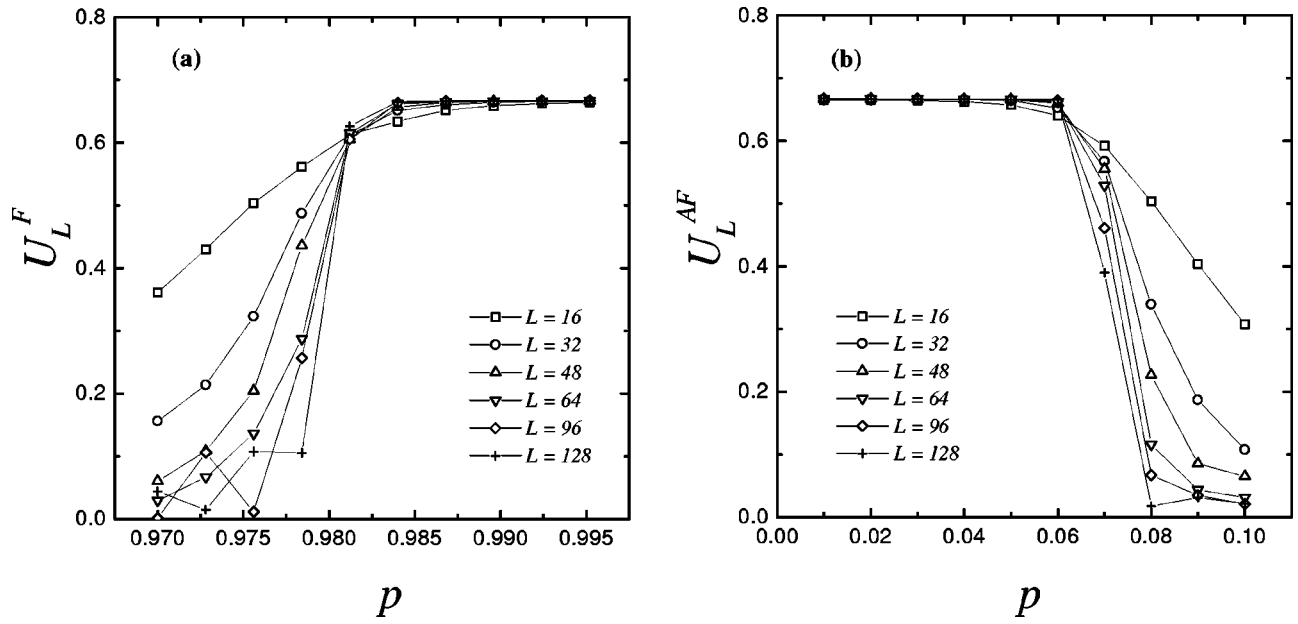


FIG. 4. Fourth-order cumulant for various system sizes as indicated in the figures. (a) The critical competition parameter is $p_c = 0.9812 \pm 0.0001$ at the transition line $P$-$F$ for $T = 1.5$. (b) At the transition line AF-$P$, for $T = 2.0$, we obtained $p_c = 0.065 \pm 0.001$.

cal value of $p$ is located in this range. The same behavior is also noted in Fig. 3(b), where the order parameter $m^{\mathrm{AF}}$ is plotted versus $1/L$, for $p$ in the range 0.050–0.070.

For a better determination of the critical parameters, we used the fourth-order cumulant intersection property [9]. The scaling relation for the fourth-order cumulant shows that, at the critical competition parameter, all curves must cross at a common point. In order to find the critical parameter, we fixed the temperature, which is measured in units of $J/k_B$, and we plotted $U_L(p)$ versus the competition parameter $p$, for various lattice sizes $L$, as shown in Figs. 4(a) and 4(b). Our estimate for the critical competition parameter at the transition line between the ordered $F$ and paramagnetic $P$ phases is $p_c = 0.9812 \pm 0.0001$, while its value at the other transition line (AF-$P$ transition line) is $p_c = 0.065 \pm 0.001$.

From the Monte Carlo simulations, we can also evaluate the critical exponents of the model. For instance, the exponent $\nu$ that is associated with the correlation length can be obtained from Eq. (19). We see that, at the critical competition parameter $p_c$, $U_L'(p_c)$ scales as $L^{1/\nu}$. Then, from the log-log plot of $U_L'(p_c)$ versus $L$ [see Fig. 5(a)], the best fit to the Monte Carlo data gives us $\nu = 1.01 \pm 0.06$, while in Fig. 5(b), the best fit gives us $\nu = 1.09 \pm 0.05$. Figure 6 shows the log-log plots of $m^F$ and $m^{\mathrm{AF}}$ as functions of $L$ at the corresponding critical points. The best fit to the data points of Fig. 6(a) furnishes the value $\beta/\nu = 0.125 \pm 0.009$ for the $F$-$P$

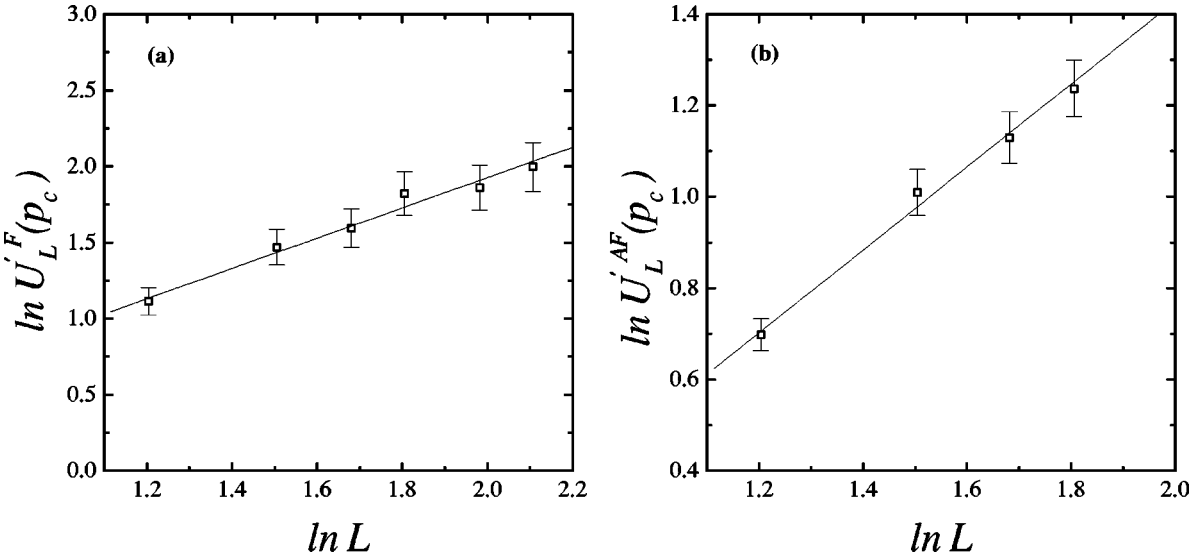


FIG. 5. Plot of $U_L'(p_c)$ versus $L$. The straight lines are the best fits to the data points. (a) At the transition line $P$-$F$, for $T = 1.5$, we obtained $\nu = 1.01 \pm 0.06$. (b) At the transition line AF-$P$, for $T = 2.0$, we obtained $\nu = 1.09 \pm 0.05$.

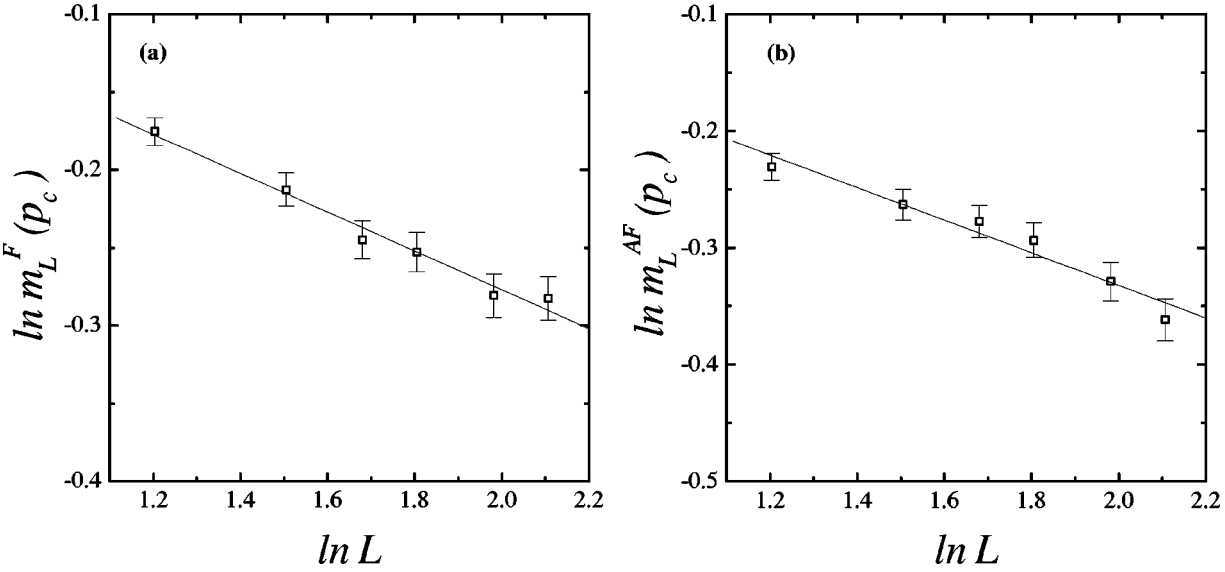


FIG. 6. Plot of $m_L(p_c)$ versus $L$. The straight lines are the best fits to the data points. (a) At the transition line $P$-$F$, for $T=1.5$, we found $\beta/\nu=0.125\pm0.009$. (b) At the transition line AF-$P$, for $T=2.0$, we found $\beta/\nu=0.13\pm0.01$.

transition, while we get the value $\beta/\nu=0.13\pm0.01$ for the AF-$P$ transition. Another critical exponent of interest is that associated with the susceptibility. From the log-log plots of $\chi^F$ and $\chi^{\mathrm{AF}}$ at their respective critical points we can find the exponent ratio $\gamma/\nu$. Figure 7(a) gives $\gamma/\nu=1.67\pm0.08$ for the $F$-$P$ transition, and Fig. 7(b) gives $\gamma/\nu=1.63\pm0.04$ for the AF-$P$ transition.

More precise values of the critical exponents can be found by collapsing the data points. For instance, we exhibit in Figs. 8 and 9 the data collapse for the order parameters $m^F$ and $m^{\mathrm{AF}}$ and for the susceptibilities $\chi^F$ and $\chi^{\mathrm{AF}}$, respectively. The data points for all the lattice sizes considered are located on two different branches: one for $\epsilon>0$ and the other for $\epsilon<0$, where $\epsilon=(p-p_c)/p_c$. At the $F$-$P$ transition line, the paramagnetic phase is given by $\epsilon<0$, while at the AF-$P$ transition line, $\epsilon>0$ characterizes the paramagnetic phase. From the slopes of these curves for large values of the parameter $\epsilon L^{1/\nu}$ we can determine the exponents $\beta$ and $\gamma$. On the other hand, from the other branches, which are related to the ordered phases, the slopes of the curves for large values of $\epsilon L^{1/\nu}$ give $\beta-\nu$ (Fig. 8) and $\gamma$ (Fig. 9). The optimal values we have found for the critical exponents employing this procedure are as follows. At the $F$-$P$ transition line $\nu=1.02\pm0.02$, $\beta=0.123\pm0.002$, and $\gamma=1.73\pm0.02$ and at the AF-$P$ transition line $\nu=1.02\pm0.02$, $\beta=0.123\pm0.003$, and $\gamma=1.73\pm0.03$. We repeated the whole process outlined above for other points along the critical lines. We summarize these results in Fig. 10, where we plotted the exponents $\nu$, $\beta$,

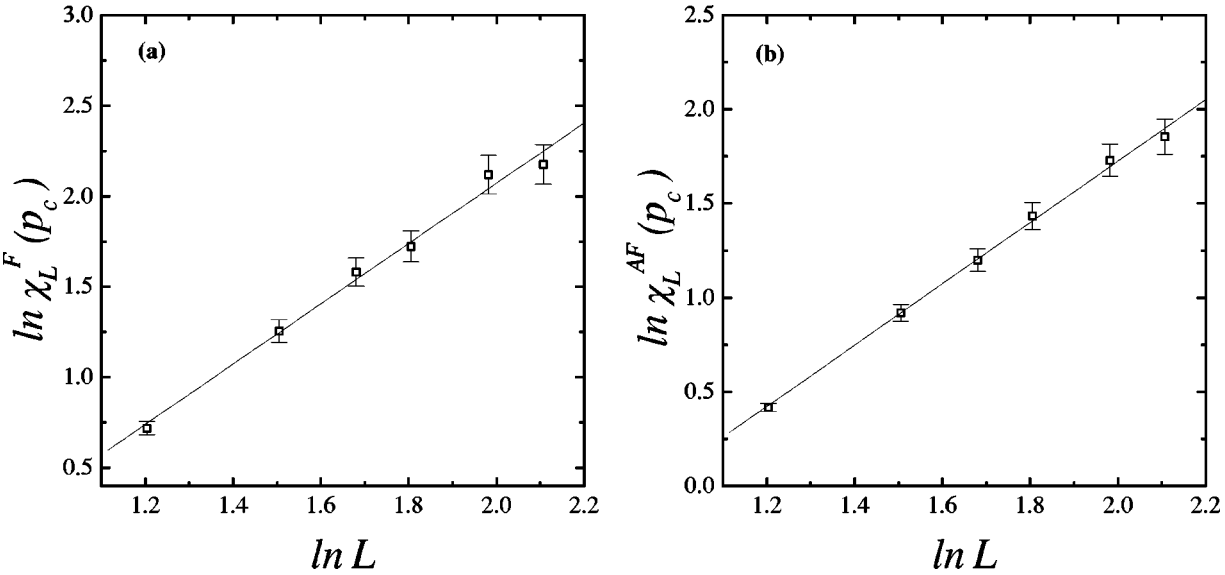


FIG. 7. Plot of $\chi_L(p_c)$ versus $L$. The straight lines are the best fits to the data points. (a) At the transition line $P$-$F$, for $T=1.5$, we found $\gamma/\nu=1.67\pm0.08$. (b) At the transition line AF-$P$, for $T=2.0$, we found $\gamma/\nu=1.63\pm0.04$.

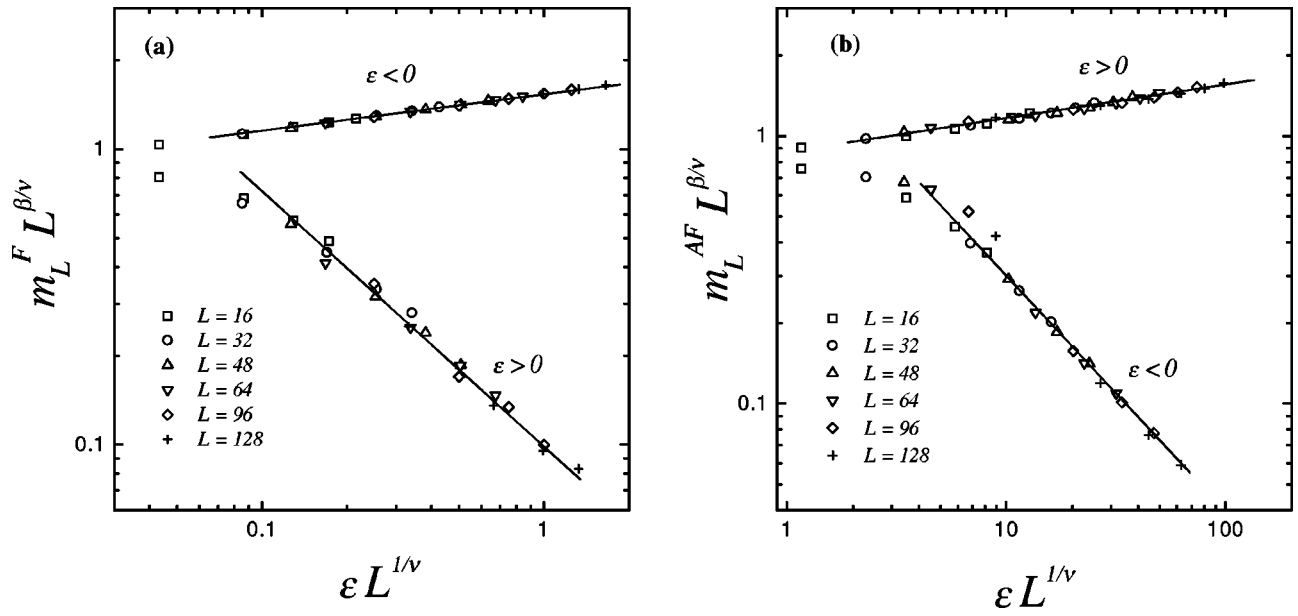


FIG. 8. Finite-size scaling (full data collapse) for the magnetization $m_L$, and for different values of $L$ as indicated in the figures. The parameter $\epsilon$ is defined by $\epsilon=(p-p_c)/p_c$. The straight lines represent the asymptotic behavior of the scaling functions. (a) At the transition line $P$-$F$, for $T=1.5$, the optimal values are $p_c=0.9812\pm0.0001$, $\nu=1.02\pm0.02$, and $\beta=0.123\pm0.002$. (b) At the transition line AF-$P$, for $T=2.0$, the optimal values are $p_c=0.065\pm0.001$, $\nu=1.02\pm0.02$, and $\beta=0.123\pm0.003$.

and $\gamma$ versus the competition parameter $p$. The left part of this figure accounts for the AF-$P$ transition line, while the right part is related to the $F$-$P$ transition line. As we can see, the values we have obtained for these critical exponents compare very well with the analogous static exponents of the equilibrium two-dimensional Ising model. The nonequilibrium mixed-spin Ising model that we have considered preserves the up-down symmetry, and this fact puts it in the same universality class as the corresponding equilibrium Ising model [11].

## V. CONCLUSIONS

We have studied a nonequilibrium mixed-spin ferromagnetic Ising model on a bipartite square lattice. Spins of magnitude $\sigma=1/2$ were put in one sublattice, while spins of mag-

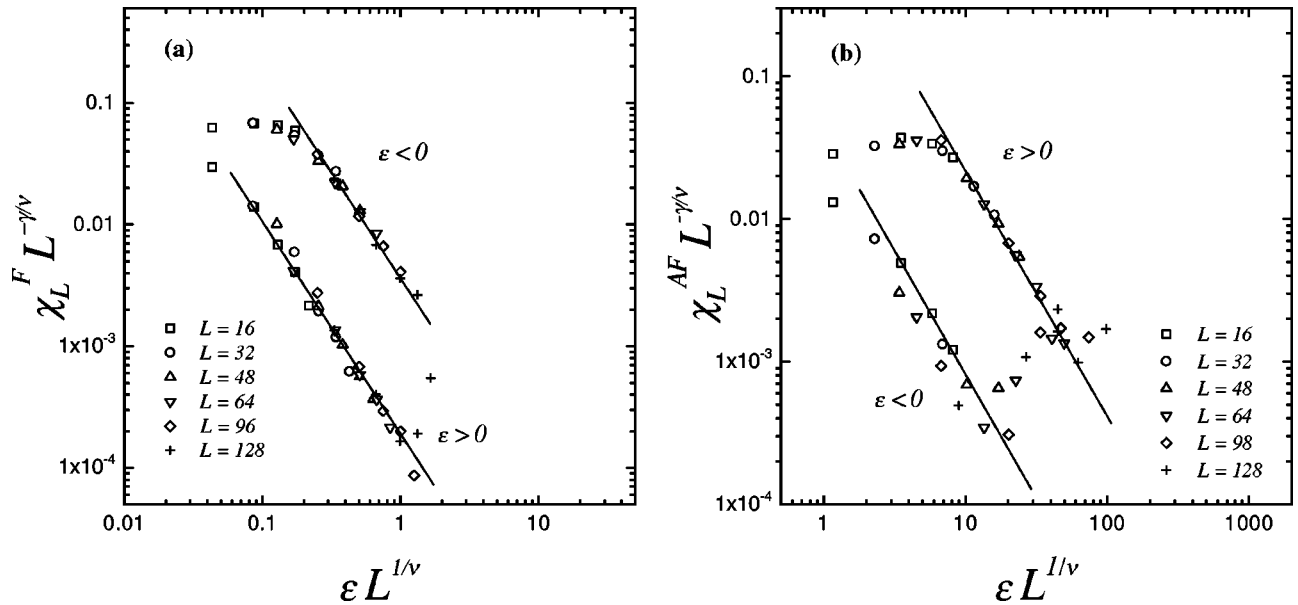


FIG. 9. Finite-size scaling (full data collapse) for the susceptibility $\chi_L$, and for different values of $L$ as indicated in the figures. The parameter $\epsilon$ is defined by $\epsilon=(p-p_c)/p_c$. The straight lines represent the asymptotic behavior of the scaling functions. (a) At the transition line $P$-$F$, for $T=1.5$, the optimal values are $p_c=0.9812\pm0.0001$, $\nu=1.02\pm0.02$, and $\gamma=1.73\pm0.02$. (b) At the transition line AF-$P$, for $T=2.0$, the optimal values are $p_c=0.065\pm0.001$, $\nu=1.02\pm0.02$, and $\gamma=1.73\pm0.03$.

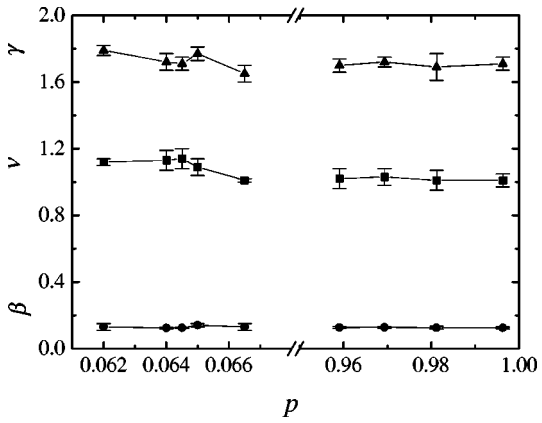


FIG. 10. Static critical exponents $\nu$, $\beta$, and $\gamma$ as functions of the competition parameter $p$. The left part of the figure accounts for the AF-$P$ transition line, while its right part is related to the $F$-$P$ transition line.

nitude $S=1$ were located in the other sublattice. The system was in contact with a heat bath at fixed temperature and, at the same time, subjected to an external flux of energy. The contact with the heat bath was simulated by the one-spin flip Glauber process with probability $p$, while the flux of energy was simulated by a process involving a simultaneous flipping of a pair of nearest neighbor spins, with probability $(1-p)$. Through Monte Carlo simulations and finite-size scaling arguments we determined the phase diagram of the model in the plane of the temperature of the heat bath versus the competition parameter $p$. We showed that the phase diagram contains three phases separated by two continuous transition lines. When the flux of energy is very small the system is ordered with the spins of both sublattices in the same direction, while for large values of the flux of energy the system is also ordered but with the spins of sublattices pointing in opposite directions. For almost all values of $p$ the phase diagram exhibits a well defined paramagnetic phase where the sublattice magnetizations vanish. We also calculated the critical exponents $\nu$, $\beta$, and $\gamma$ along these two critical lines, and showed that this nonequilibrium model is in the same universality class as the equilibrium Ising model in two dimensions.

## ACKNOWLEDGMENTS

This work was partially supported by the Brazilian agencies CAPES, CNPq, and FINEP.

[1] J. Marro and R. Dickman, *Nonequilibrium Phase Transitions in Lattice Models* (Cambridge University Press, Cambridge, England, 1999).
[2] *Nonequilibrium Statistical Mechanics in One Dimension*, edited by V. Privman (Cambridge University Press, Cambridge, England, 1996).
[3] R. J. Glauber, J. Math. Phys. **4**, 294 (1963).
[4] M. Godoy and W. Figueiredo, Phys. Rev. E **61**, 218 (2000).
[5] K. Kawasaki, in *Phase Transitions and Critical Phenomena*, Vol. 2, edited by C. Domb and M. S. Green (Academic, London, 1972), p. 443.
[6] T. Tomé and M. J. de Oliveira, Phys. Rev. A **40**, 6643 (1989).
[7] W. Figueiredo and B. C. S. Grandi, Braz. J. Phys. **30**, 58 (2000).
[8] K. Binder, in *Finite-Size Scaling and Numerical Simulation of Statistical Systems*, edited by V. Privman (World Scientific, Singapore, 1990).
[9] K. Binder and D. W. Heermann, *Monte Carlo Simulation in Statistical Physics. An Introduction*, 3rd ed. (Springer, Berlin, 1997).
[10] R. G. Bowers and B. Y. Yousif, Phys. Lett. **96A**, 49 (1983).
[11] G. Grinstein, C. Jayaprakash, and Yu He, Phys. Rev. Lett. **55**, 2527 (1985).